Published in final edited form as:

Oncogene. 2023 March ; 42(10): 759–770. doi:10.1038/s41388-022-02587-1.

Muc4 loss mitigates epidermal growth factor receptor activity essential for PDAC tumorigenesis

Rakesh Bhatia[1], **Jawed Akhtar Siddiqui**[1], **Koelina Ganguly**[1], **Christopher M Thompson**[1], **Andrew Cannon**[1], **Abhijit Aithal**[1], **Naveenkumar Perumal**[1], **Shailendra K Maurya**[1], **Xiaoqi Li**[1], **Jesse L. Cox**[2], **Channabasavaiah B Gurumurthy**[3], **Satyanarayana Rachagani**[1], **Maneesh Jain**[1,4], **Mohd. Wasim Nasser**[1], **Surinder K. Batra**[1,4,5,*], **Sushil Kumar**[1,4,*]

[1]Department of Biochemistry and Molecular Biology, University of Nebraska Medical Center, Omaha, NE, U.S.A.

[2]Department of Pathology and Microbiology, University of Nebraska Medical Center, Omaha, NE, U.S.A.

[3]Department of Pharmacology and Experimental Neuroscience, University of Nebraska Medical Center, Omaha, NE, U.S.A.

[4]Fred and Pamela Buffett Cancer Center, Omaha, NE, U.S.A.

[5]Eppley Institute for Research in Cancer and Allied Diseases, University of Nebraska Medical Center, Omaha, NE, U.S.A

Abstract

Mucin4 (MUC4) appears early during pancreatic intraepithelial neoplasia-1 (PanIN1), coinciding with the expression of epidermal growth factor receptor-1 (EGFR). The EGFR signaling is required for the onset of Kras-driven pancreatic ductal adenocarcinoma (PDAC); however, the players and mechanisms involved in sustained EGFR signaling in early PanIN lesions remain elusive. We generated a unique *Esai*-CRISPR-based Muc4 conditional knockout murine model to evaluate its effect on PDAC pathology. The Muc4 depletion in the autochthonous murine model carrying K-ras and p53 mutations (K-ras^{G12D}; TP53^{R172H}; Pdx-1cre, KPC) to generate the KPCM4$^{-/-}$ murine model showed a significant delay in the PanIN lesion formation with a significant reduction (p<0.01) in EGFR(Y1068) and ERK1/2 (T202/Y204) phosphorylation. Further, a significant decrease (p<0.01) in Sox9 expression in PanIN lesions of KPCM4$^{-/-}$ mice suggested the impairment of acinar-to-ductal metaplasia in Muc4-depleted cells. The biochemical analyses demonstrated that MUC4, through its juxtamembrane EGF-like domains, interacts with the EGFR ectodomain, and its cytoplasmic tail prevents EGFR ubiquitination and subsequent

[*]**Correspondence**: Sushil Kumar or Surinder K Batra, Department of Biochemistry and Molecular Biology, 985870, University of Nebraska Medical Center, Omaha, Nebraska, 68198-5870, U.S.A.; Tel: 402-559-3138, Fax: 402-559-6650, skumar@unmc.edu or sbatra@unmc.edu.

Author contributions. R.B. performed biochemical analysis and wrote the manuscript. R.B, J.A.S., N.K.P., S.K.M., and X. L. generated and characterized KPCM4$^{-/-}$ murine model. K.G. performed I.H.C. experiments. C.M.T. and A.C. performed bioinformatics analysis. A.A. generated the MUC4 monoclonal antibody. J.L.C. scored I.H.C. slides. C.S.B. helped in the generation of Muc4 COIN mice. S.R., M.J., M.W.N., provided inputs in murine model studies. S.K. conceived the idea and designed the experiments. S.K and S.K.B supervised the project and approved the manuscript.

Competing interests. S.K.B. is a founder of Sanguine Diagnostics and Therapeutics, Inc. Other authors have no competing interests to declare.

proteasomal degradation upon ligand stimulation, leading to sustained downstream oncogenic signaling. Targeting the MUC4 and EGFR interacting interface provides a promising strategy to improve the efficacy of EGFR-targeted therapies in PDAC and other MUC4-expressing malignancies.

Keywords

Pancreatic ductal adenocarcinoma; Acinar-to-ductal metaplasia (ADM); Epidermal growth factor receptor; Mucin 4; *Esai*-CRISPR

Introduction

Constitutive activation of mutant Kras is a major cause of the onset of pancreatic ductal adenocarcinoma (PDAC). However, the early molecular events involved in tumorigenesis remain inadequately defined. The first noticeable event at the cellular level after Kras activation in murine models is the transdifferentiation of pancreatic acinar cells into ductal phenotype, known as acinar-to-ductal metaplasia (ADM). The activating Kras mutations irreversibly lock acinar cells undergoing ADM into a ductal phenotype [1], further progressing to more complex ductal structures characterized as pancreatic intraepithelial neoplasia (PanIN) [2, 3]. Besides the important contribution of Krüppel-like factor 4 (KLF4) and SRY-box transcription factor 9 (SOX9) in PDAC initiation [4, 5], earlier studies on ADM suggest its primary dependence on epidermal growth factor receptor-1 (EGFR) activation [6-8]. The appearance of metaplastic ducts [9] increases significantly upon treatment with EGFR-ligands like EGF and TGF-α *in vivo* [6, 10]. The EGFR and its ligands are significantly upregulated [7, 11] even before tumor initiation in mutant Kras-expressing mice, suggesting that activation of EGFR precedes PDAC tumorigenesis [7]. Further, consistently lower activation of Ras/MEK/ERK and PI3K/AKT signaling and the absence of early PanINs in K-Ras^{G12D}; EGFR knockout mice [6, 12] establish the essential requirement of EGFR signaling in PDAC initiation. Unlike malignancies such as lung, brain, and colon cancers, where EGFR mutations lead to its constitutive activation, these mutations are infrequent and rare in PDAC [13]. Instead, the mechanism of prolonged oncogenic signaling is critical for PDAC initiation, involving membrane stabilization and altered trafficking of EGFR upon ligand stimulation [14, 15]. However, the mechanisms and molecules responsible for prolonged EGFR signaling during PDAC tumorigenesis and progression are poorly understood.

Another hallmark of PDAC is the *de novo* expression of mucins during the initial stages of the disease. Mucin expression and secretion are the characteristic feature of epithelial cells but are generally considered *inert* molecules that are merely involved in establishing a mucinous barrier [16, 17]. However, studies have shown that these mega-Dalton glycoproteins can also contribute to the aggressiveness of cancer [18, 19]. Among all mucins, MUC4 is unique due to the presence of multiple functional domains, divided into N-terminal alpha and C-terminal beta domains based on the putative cleavage site. The N-terminal alpha region contains a glycosylated tandem-repeat region, nidogen-like domain (NIDO), adhesion-associated domain in MUC4, and other proteins (AMOP). In contrast, the

beta region contains von Willebrand factor type D (vWD), three juxtamembrane EGF-like domains, and a cytoplasmic tail (CT) [20]. MUC4 is absent in normal and inflamed pancreas but expressed early upon oncogenic insult. In PDAC, MUC4 has been associated with proliferation, chemoresistance, metastasis, and poor survival [19]. However, the majority of these studies focused on the advanced stages of PDAC using cell lines, and its role during PDAC inception remains elusive due to the lack of appropriate murine models.

In the present study, we generated a pancreas-specific Muc4 conditional knockout mouse model using a novel *conditional-by-inversion* (COIN) strategy by inserting an inversion cassette containing a stop codon and 3X polyA in the first intron. Surprisingly, conditional Muc4 knockout ($M4^{-/-}$) in a $Kras^{G12D}$; $TP53^{R172H}$; Pdx1-Cre (KPC) background significantly delayed the appearance of PanIN lesions. Further investigations showed a significant decrease in EGFR and downstream ERK1/2 activity in the pancreatic tissues of $KPCM4^{-/-}$ mice. Mechanistically, MUC4 physically interacts with EGFR in a ligand-dependent manner, sustaining the oncogenic signaling required for ADM and PanIN lesion formation. MUC4 maintains EGFR stability on the cell surface by inhibiting its ubiquitination-mediated degradation upon ligand stimulation.

Materials and Methods

Generation of conditional MUC4 knockout (KO) mouse model:

The Muc4 genomic region has an unusually complex exon-intron structure. Exon 2 (8.4 kb) contains most of the coding sequence and would be ideal to flox to ensure the deletion of the significant part of the protein. But the traditional approaches using a one-targeting construct would be very challenging to flox such a large exon [21, 22]. To address this issue, we employed the conditional by inversion (COIN) strategy [23]. Following the *Easi*-CRISPR strategy, a single-stranded DNA cassette was inserted into the genome. The sgRNA (CTAACCACTTAAGTGGTGCA) chosen for knocking in the DNA cassette targets the Muc4 gene at 2308 bases upstream of the exon 2. (See Supplementary Material for details).

Genetically engineered mouse models of PDAC:

All experimental animal models and protocols were approved by the Institutional Animal Care and Use Committee (IACUC) at the University of Nebraska Medical Center (UNMC). The $Kras^{+/-LSLG12D}$ mice were bred with mice carrying Pdx-1cre (KC) or both $TP53^{+/-LSLR172H}$ and Pdx-1cre (KPC) in C57BL/6 background. The pancreas-specific conditional MUC4 knockout ($KPCM4^{-/-}$) animals were generated by breeding $M4^{COIN/COIN}$ mice with KPC mice. Both male and female mice were used to investigate the role of Muc4 in PDAC pathology. For animal studies based on tumor weight compared to the age group, n=3 (only for more than 30 weeks of age) to n=10 animals were used. Animals were humanely euthanized at the indicated time points or closer to morbidity. Dissected pancreata were processed for RNA, protein, and histological analysis using the standard protocols.

Cerulein treatment for inflammation-driven ADM:

Both male and female KC and wild-type mice (6-8 weeks) were treated with cerulein (75 μg/kg) by giving eight intraperitoneally (i.p.) injections per hour for two alternate days as per the staggered protocol [24]. Considering the last injection as day 0 of treatment, mice were humanely euthanized at 2- and 7-days post-injection. The tissues were harvested, buffered formalin-fixed, and processed for histological analysis.

Cell lines and primary acinar cell culture:

Br404, Br451, and Br317 mouse PDAC cell lines were derived from KPC and KPCM4$^{-/-}$ mice pancreata and authenticated for Kras^{G12D} and TP53^{R172H} mutations. Mouse acinar cell line (266.6) and human PDAC cell lines, such as CD18/HPAF, Colo357, and AsPC-1, were procured from American Type Culture Collection (ATCC), authenticated by STR profiling and maintained/stored frozen as per standard protocol. The AsPC-1 cell lines expressing a control vector or the different MUC4β subunit constructs were prepared and maintained in antibiotic selection using 100 μg/ml of zeocin. On the other hand, CD18/HPAF cells with stable shRNA-mediated MUC4 KD were generated and maintained in 2 μg/ml of puromycin.

Quantification and statistical analysis:

Histology scores representing intensity and percentage area covered for different antibodies on animal tissues were compared using a student's t-test. Densitometry on western blots was performed using ImageJ1.52s software, and the student's t-test determined statistical significance from three independent experiments. To test the hypothesis, power analysis for difference in tumor weight was performed considering normal distribution, two-tailed analysis and significance less than 0.05 ($p<0.05$) and power of 0.8. Results with p-values less 0.05 were considered as statstically significant. Confocal data was quantified from patient tissues using ZEN 2.3 SP1 black edition software.

Supplementary methods:

Additional experimental methods, including bioinformatics analysis [25] and key resources (supplementary Table 1), are available in the supplementary information.

Results

Conditional genetic ablation of Muc4 significantly delays PanIN lesion formation.

To investigate the contribution of early expression of Muc4 in PDAC biology, we conditionally ablated Muc4 utilizing a conditional by inversion (COIN) strategy [23] using the *Easi*-CRISPR method [26, 27]. The Muc4 genomic organization is unusually complex. Of the 25 exons, exon 2 contains >70% of the coding sequence (8484 out of 11970 bases) that is mostly repetitive (Fig. S1), and the traditional approaches using a one-targeting construct would be very challenging to flox such a large exon [21, 22]. Therefore, we employed the COIN strategy [23]. Upon Cre recombinase-mediated inversion, the cassette is flipped to provide a strong splice acceptor site for exon 1, leading to premature termination and Muc4 depletion (Figs. 1A, S1, S2A, and S2B). The Muc4^{COIN} mice were bred with

KPC mice to generate KPCMuc4$^{-/-}$ (KPCM4$^{-/-}$) mice (Fig. 1A). Validation on pancreatic tissues, cell lines derived from KPC/KPCM4$^{-/-}$ pancreas (Figs. 1C, S2C, and S2D), mouse tail and cell line genomic DNA (Fig. S2E) confirmed the successful MUC4 deletion and a plausible nonsense-mediated decay of the recombined transcript after inversion. The *in-situ* hybridization confirmed complete Muc4 depletion in KPCM4$^{-/-}$ mice pancreatic lesions using specific probes targeted to exon 2 (Fig. 1B).

The KPC and KPCM4$^{-/-}$ animals were followed for tumor progression. Interestingly, we observed a significant delay in tumor initiation in KPCM4$^{-/-}$ mice compared to KPC littermates. The KPC animals developed PanIN lesions at 5-weeks and tumors by 20 weeks, as shown in previous studies [28]. However, PanIN lesions developed significantly later in KPCM4$^{-/-}$ mice, appearing around 15 weeks of age, and the majority of mice survived up to 60 weeks postnatally (Figs. 1D and 1E). This delay in initiation was associated with significantly lower pancreas weight (Fig. 1F) and the ratio of the pancreas to body weight (Fig. 1G) in KPCM4$^{-/-}$ mice compared to the KPC mice. As conditional Muc4 depletion significantly delays the onset of PanIN lesion formation, we subsequently focused on the role of Muc4 in PDAC initiation.

Muc4 ablation significantly reduced EGFR-mediated signaling.

To understand how Muc4 deletion delayed PanIN formation, we performed gene ontology enrichment analysis in MUC4 high- and low- expressing patient samples using the TCGA dataset and observed the enrichment of SH2 domain binding function, depicting its involvement in tyrosine kinases-driven signaling pathways (Fig. 2A). Next, we correlated TCGA MUC4 expressing samples with matched reverse-phase proteomic data from the TCGA patients and observed a significant correlation (Rho= 0.22 and p= 0.029) between MUC4 transcript and pEGFR Y1068 levels, suggesting a higher activation of EGFR signaling in the presence of MUC4 (Fig. 2B). This correlation of MUC4 in EGFR signaling was further validated *in vivo* by a significant decrease in pEGFR (Y1068) and pERK1/2 (T202/Y204) levels in histology-matched (Figs. 2C and 2D), KPCM4$^{-/-}$ (30-40 weeks) PanIN lesions compared to KPC mice (11-20 weeks), as well as in age-matched lesions (Fig. S3A). Further, we found a significant reduction in the levels of pEGFR (Y1068) and downstream ERK1/2 phosphorylation (T202/Y204) in the pancreatic lysates from KPCM4$^{-/-}$ compared with KPC mice (Fig. 2E). To rule out the possibility that the lower phosphorylation status of EGFR is due to lower ligand expression in KPCM4$^{-/-}$ animals, we first analyzed the expression levels of different EGFR-ligands in a cellularity-corrected PDAC TCGA dataset. Interestingly, heparin-binding EGF-like growth factor (HBEGF) and amphiregulin (AREG) were the two most significantly expressed EGFR-ligands, followed by transforming growth factor-alpha (TGFα) and epiregulin (EREG). The EGF, betacellulin, and epigen were not expressed to noticeable levels (Fig. 2F). This data was further confirmed using two different PDAC microarray data sets, which also showed higher expression of HBEGF and AREG; however, total EGFR levels remain unaltered (Figs. S3B-S3E). Interestingly, the expression levels of four highly expressed EGFR-ligands were not significantly different in the KPC and KPCM4$^{-/-}$ mice (Fig. 2G). Concurrently, we did not observe any change in the expression of other mucins (Figs. S4A and S4B), including Muc1, Muc5ac, and Muc16 in KPCM4$^{-/-}$ pancreatic tissues and cell lines, suggesting that

lower EGFR phosphorylation status in the PanIN lesions is primarily driven by the lack of Muc4 expression (Figs. S4C and S4D). Together, the delay in tumor initiation and decrease in the activation status of EGFR and ERK1/2 in PanIN lesions of KPCM4$^{-/-}$ mice suggest that Muc4 significantly enhances the EGFR signaling essentially required for Kras-driven PDAC tumorigenesis [6, 7].

Decreased EGFR activity upon Muc4 depletion reduces Sox9 expression and ADM.

The Sox9 expression is critical for ductal transdifferentiation of pancreatic acinar cells [4], which in PDAC is regulated by multiple mechanisms [29]. Interestingly, Sox9 expression was significantly reduced in ADM and PanIN1 and −2 lesions in KPCM4$^{-/-}$ mice (Figs. 3A and 3B). A significant decrease in Sox9 and CK19 expression in the tissues and tissue lysates of the pancreata from KPCM4$^{-/-}$ compared to KPC mice further corroborated these findings (Fig. 3C and Fig. S5A). However, we did not observe any change in Klf4 expression (Figs. S5B and S5C), another molecule involved in ADM, suggesting that the Muc4-mediated increase in EGFR activity facilitates ADM by upregulating Sox9 expression. Further, the ducts showed significantly lower Ki67 staining in KPCM4$^{-/-}$ vs. KPC pancreas (Figs. 3D and Fig. S5D). In line with a previous report [30], we observed a substantial decrease in SOX9 expression after erlotinib treatment in the PDAC cell line, CD18/HPAF (Fig. 3E), in the presence of HBEGF. To further evaluate the dependence of SOX9 on MUC4, we silenced MUC4 (Fig. 3F) in CD18/HPAF cells and treated them with HBEGF. As expected, in the absence of MUC4, HBEGF failed to upregulate SOX9 expression to the level of MUC4-proficient cells, demonstrating the importance of MUC4 in EGFR-mediated regulation of SOX9 (Fig. 3G). We next performed an *ex vivo* experiment by transducing primary pancreatic acinar cells from Kras$^{LSLG12D/+}$ (K) and Kras$^{LSLG12D/+}$ MUC4$^{COIN/COIN}$ (KM) mice with GFP-expressing Cre-adenovirus (Ad-cre-GFP) and treated them with mHBEGF (Fig. 3H). Compared to the K mice, acini from KM mice showed fewer ductal structures and reduced growth (GFP expression) after mHBEGF treatment (Figs. 3I and 3J), as well as lower phosphorylation status of EGFR (Y1068) and ERK1/2 (T202/Y204) and reduced expression of Sox9 (Fig. 3K). Collectively, our results suggest that MUC4 potentiates EGFR signaling upon ligand treatment, which increases the expression of Sox9, promoting ADM and PanIN lesion formation.

Muc4 expression correlates with higher EGFR activation during ADM.

As Muc4 expression appears early during ADM, we investigated the correlation between Muc4 and pEGFR (Y1068) in early PanINs in a comparatively slow-progressing KC murine model. The IHC analysis revealed significant co-expression of Muc4 and pEGFR (Y1068), especially in the trans-differentiation zone (ADM) and in early PanIN lesions of KC mice (Figs. 4A and 4B). Correlation of histology score demonstrated a significant correlation between Muc4 and pEGFR (Y1068) in PanIN-1 (r= 0.558; p= 0.05) (Fig. 4C) and moderate correlation in PanIN-2 (r= 0.227) lesions (Fig. 4D), suggesting that early lesions express both Muc4 and EGFR. Previous studies have shown that pancreatic inflammation accelerates the formation of ADM and PanIN lesions due to increased infiltration of macrophages that contribute to EGFR ligands [31, 32]. Therefore, we analyzed Muc4 and pEGFR (Y1068) co-expression in KC mice after cerulein-induced pancreatic inflammation (Fig. 4E). Interestingly, KC mice showed much stronger expression and correlation (r= 0.654; p= 0.07)

of Muc4 and pEGFR (Y1068) in transdifferentiating zones after cerulein treatment (Figs. 4F and 4G). To further analyze the clinical relevance of MUC4, we analyzed the co-expression of MUC4 and pEGFR (Y1068) in Whipple samples from PDAC patients. Interestingly, we observed a strong co-localization of MUC4 and pEGFR (Y1068) (Fig. 4H) (co-localization coefficient = 0.405; p = 0.0001) (Fig. 4I) in PanIN lesions (Fig. S6A) associated with the PDAC tumor tissues. Together, this data demonstrates that MUC4 expression and EGFR phosphorylation correlate significantly in ADM, early PanIN lesions, and pancreatic tumor tissues.

MUC4 physically interacts and stabilizes EGFR on the plasma membrane upon activation.

Based on the co-localization of MUC4 and pEGFR (Y1068) in patient samples and the presence of three EGF-like domains in MUC4, we evaluated the possibility of physical interaction between MUC4 and EGFR, utilizing PDAC cell lines, CD18/HPAF and Colo357. First, unlike EGF, the HBEGF and AREG treatments led to sustained EGFR phosphorylation at serine (S1046/7) and tyrosine (Y1068) residues in both cell lines. The EGF treatment showed peak phosphorylation in the first 30 min; however, HBEGF maintained higher phosphorylation status up to 6h. Similarly, AREG treatment induces maximum EGFR phosphorylation at 2 h, which stayed significantly high up to 6h in both Colo357 (Figs. 5A and 5B) and CD18/HPAF (Figs. S6B and Fig. 5C) cells. Next, we immunoprecipitated EGFR in the presence of HBEGF and probed for MUC4 as well as MUC1 and MUC5AC to ascertain the specificity of the EGFR interaction. Interestingly, compared to MUC1 and MUC5AC (Figs. S6C and S6D), MUC4 interacted with EGFR in both CD18/HPAF and Colo357 cell lines in a ligand-dependent manner (Fig. 5D). Unlike a previous report [33], we did not observe MUC1 Co-IP with EGFR, which might be due to the negligible galectin-3 in the culture supernatant (Fig. S6E), which is required for MUC1 and EGFR interaction. Next, we performed reciprocal Co-IP using MUC4 tandem repeat (8G7) and β-subunit (6E8) antibodies. Unlike the tandem repeat antibody, the anti-MUC4β (M4β) subunit antibody showed robust EGFR and pEGFR (Y1068) enrichment upon stimulation with HBEGF (Fig. 5E). Further, HBEGF and AREG treatments resulted in higher EGFR pulldown than EGF treated and untreated controls (Fig. 5F), suggesting that phosphorylated EGFR preferentially interacts with MUC4. Moreover, MUC4-silenced cells exhibited lower pEGFR (Y1068) levels than control cells, suggesting that MUC4 stabilizes pEGFR after ligand treatment (Fig. 5G).

Next, we investigated the impact of MUC4 on the fate of pEGFR. The MUC4 KD (ShMUC4) in CD18/HPAF cells led to a significant decrease in EGFR phosphorylation (Y1068, S1046/7) up to 60 min compared with MUC4-proficient (MUC4Scr) cells in response to HBEGF (Figs. 5H and 5I) and AREG treatment (Figs. 5J and 5K). The decrease in the phosphorylation status of downstream effectors such as FAK, AKT, and ERK1/2 in treated ShMUC4 cells (Fig. 5L) further cemented the role of MUC4 in sustaining EGFR signaling in PDAC. Similar results were observed in murine cell lines derived from KPCM4$^{-/-}$ PDAC tissues, whereas the KPC-derived cell line showed sustained EGFR phosphorylation compared to the KPCM4$^{-/-}$ cells (Fig. S7A). Previously, MUC4 has been shown to interact with HER2 [34], a ligand-less receptor expressed during advanced stages of PDAC development [35]. Therefore, we examined whether HER2 mediates the MUC4-

EGFR interaction. The HER2-proficient (HER2Scr) and KD (ShHER2) cells (Fig. S7B) in the presence of HBEGF showed no difference in EGFR Co-IP with MUC4 (Fig. S7C), suggesting that the MUC4-EGFR interaction is HER2-independent.

MUC4 cytoplasmic tail inhibits EGFR ubiquitination for sustained signaling.

Next, we sought to identify the region of MUC4 that interacts with EGFR and the mechanism of increased stability of pEGFR. We focused on MUC4β as it contains three EGF-like domains (Fig. S7D) and generated 3xflag-tagged truncated MUC4β constructs, deleting one domain at a time (Figs. 6A, S7E, S7F, and S8A). The reciprocal Co-IP demonstrated a physical interaction between MUC4β and EGFR upon ligand stimulation (Fig. 6B). The domain deletion constructs showed that MUC4 and EGFR interaction is stabilized by the second and third juxtamembrane EGF-like domains of MUC4 (Fig. S8B). For reciprocal Co-IP, we co-transfected myc-tagged full-length EGFR and its extracellular domain [36] along with 3xflag-tagged MUC4β. The Co-IP with Flag antibody demonstrated that MUC4 interacts with the EGFR extracellular domain (Fig. 6C). The MUC4β-transfected cells showed increased EGFR phosphorylation at indicated time points, suggesting that the MUC4β is sufficient for sustaining prolonged EGFR activation (Fig. 6D). As MUC4β interacts with the EGFR extracellular domain and maintains EGFR activity, we analyzed pEGFR stability on purified plasma membrane fraction from MUC4β-transfected cells. Unlike vector controls, MUC4β-expressing cells treated with HBEGF demonstrated a significantly higher pEGFR stability, especially in the plasma membrane fraction (Figs. 6E and 6F), suggesting that MUC4 interacts with EGFR through its EGF-like domains in a ligand-dependent manner and maintains pEGFR activity on the plasma membrane.

Previous studies have shown that the plasma membrane stability of EGFR is altered by the ubiquitination status of its tyrosine kinase domain; therefore, we analyzed pEGFR ubiquitination in cells with MUC4 KD. The MUC4Scr and KD cells were treated with HBEGF, and EGFR ubiquitination was analyzed in the EGFR-immunoprecipitated fraction. Compared to the MUC4Scr cells, KD cells exhibited a substantial increase in EGFR ubiquitination upon ligand treatment (Fig. 6G), suggesting that MUC4 prevents pEGFR ubiquitination, hence subsequent degradation. We further analyzed the role of the MUC4β region in EGFR ubiquitination by designing two more constructs (Figs. 6H and S8C), deleting either MUC4CT (MUC4βΔCT, ectodomain) and MUC4-CT (only CT). The Co-IP experiment demonstrated that EGFR only interacted with MUC4β and MUC4βΔCT but not with the MUC4-CT (Fig. 6I). We then expressed these constructs in the presence of the proteasomal inhibitor MG132 and found a substantial increase in EGFR ubiquitination in cells transfected with both MUC4βΔCT and MUC4-CT (Fig. 6J), suggesting the requirement of both MUC4 ectodomain and CT to prevent EGFR ubiquitination. These results suggest a model where the MUC4 ectodomain interacts with and anchors EGFR on the plasma membrane, and the CT inhibits EGFR ubiquitination. We cloned and transfected the mouse MUC4β subunit consisting of three EGF-like domains in the 266.6 cells and analyzed Sox9, CK-19, and amylase expression in the presence and absence of mHBEGF. The MUC4β-expressing 266.6 cells treated with mHBEGF demonstrated a significant increase in CK-19 and Sox9 expression (Fig. S8D), indicating that the MUC4β subunit is involved in increased EGFR activity leading to Sox9 expression and ductal phenotype.

Collectively, the data suggest that MUC4β interacts with EGFR and maintains its stability by inhibiting its ubiquitin-mediated degradation upon ligand stimulation, leading to ADM driving PDAC initiation (Fig. 6K).

Discussion

Studies from PDAC cell line-driven *in vitro* and orthotopic model systems have demonstrated the role of mucins in PDAC pathology beyond biomarkers or passenger molecules. Pancreas-specific depletion of Muc4 using Pdx-1 Cre in a well-defined PDAC autochthonous murine model with $Kras^{G12D}$ and $TP53^{R172H}$ mutations [37, 38] demonstrated a significant delay in neoplastic initiation. Investigating the mechanism, we observed a significantly reduced phosphorylation of EGFR and downstream ERK1/2 signaling, which are critical for PDAC initiation in the presence of constitutively active Kras, suggesting that Muc4 is imperative for these signaling events.

Multiple studies investigating PDAC initiation have demonstrated that acinar cells expressing mutant $Kras^{G12D}$ generate PanINs through ADM. The EGFR signaling regulates the differentiation, maintenance, and progression of these neoplastic lesions [39]. Supporting these studies, Siveke et al. demonstrated that pancreas-specific activation of EGFR and RAS signaling results in faster PanIN formation and disease aggressiveness [40]. This EGFR hyperactivity and sustained signaling are significant in cancers like PDAC, where the EGFR is rarely mutated. The role of sustained EGFR signaling for ADM is further established by pancreas-specific transgenic overexpression of EGFR-ligands such as TGFα and AREG [10, 41]. However, these previous studies did not provide mechanistic insights for increased EGFR signaling in ADM and PanIN lesions. Interestingly, Muc4 expression, also regulated by mutated K-Ras [42], appears early during PDAC initiation [28], coinciding with EGFR activation. Our results suggest that early Muc4 expression is central to sustained EGFR signaling during PDAC initiation and increased expression of Sox9, a crucial transcriptional regulator of ADM upon Kras mutation. The cellularity-corrected TCGA and microarray datasets demonstrated that HBEGF and AREG are the predominant EGFR-ligands expressed in PDAC, which explains why the pancreas-specific ablation of ADAM17, a sheddase involved in the cleavage of transmembrane HBEGF, and AREG, recapitulates the phenotype of EGFR KO mice with no PanIN lesion formation [7]. Our study has also shown prolonged activation of EGFR by HBEGF and AREG. Notably, HB-EGF and AREG increased MUC4 and EGFR interaction in PDAC cells.

Next, we demonstrated that the MUC4 beta domain, especially juxtamembrane EGF-like domains, is sufficient for EGFR interaction. A recent study by Wang et al. showed angiogenin, a pancreatic ribonuclease, as a high-affinity EGFR ligand that binds and activates downstream signaling [43]. Angiogenin carries an EGF-like sequence moiety, which is also present in the second EGF-like domain in MUC4. However, our domain deletion studies suggest that the MUC4 and EGFR interaction starts at the first two juxtamembrane EGF-like domains and is further stabilized by the second and third EGF domains. In addition, the short MUC4 CT prevented EGFR ubiquitination after ligand binding, which delayed its internalization and degradation, leading to sustained signaling. This MUC4 CT-mediated inhibition of EGFR ubiquitination is plausibly through steric

hindrance to ubiquitin ligase (c-Cbl) recruitment or Grb-2-mediated mechanisms, which is an ongoing study in our laboratory. Therefore, MUC4 extracellular and CT domains act cooperatively, in which the EGF-like domain interacts and anchors EGFR to the plasma membrane in a ligand-dependent manner, and the CT prevents EGFR ubiquitination. Likewise, signal-transducing adaptor family member-2 (STAP-2) and sortilin-1 have also been shown to stabilize EGFR signaling either by altering its ubiquitination or internalization in prostate and lung cancers, respectively [44, 45]. Interestingly, previous studies have shown MUC4 interaction with other EGFR family members, Her2 and Her3, in PDAC [34, 46]. However, we have demonstrated that MUC4 and EGFR interact independently of Her2, which is expressed later during PDAC progression (PanIN III stage). Therefore, MUC4 interaction with other EGFR family members may be relevant during the later stages of PDAC.

In the present study, we predominantly focused on the MUC4 beta region. However, the N-terminal part of MUC4 with extensive glycosylation can also participate in PDAC initiation. Indeed, overexpression of glycan epitope CA19.9, also present on MUC4, in mouse pancreas led to severe acute pancreatitis [47]. It is tempting to speculate that the MUC4 N-terminal region promotes inflammatory response and facilitates the recruitment of macrophages producing EGFR ligands, leading to ligand-dependent interaction of the MUC4-beta domain with EGFR and sustaining EGFR activation. Nonetheless, our study has raised many intriguing questions about apical-basal polarity and how the glycocalyx modulates plasma membrane dynamics. For example, mucins are expressed at the apical surface and receptor tyrosine kinases are restricted to the basal surface of epithelial cells, and the loss of polarity is a relatively late event in the oncogenic cascade. Then, how do MUC4 and EGFR interact early to facilitate sustained EGFR signaling? In this regard, the ADM process is unique, as the metaplastic cells start to lose their polarity during the process of dedifferentiation, and studies have shown that reduced expression of LKB1 leads to loss of both acinar cell polarity and tight junctions [48], which may bring MUC4 and EGFR together early during ADM and PDAC initiation. Similarly, our study calls for extensive investigations of glycocalyx-mediated mechanisms and the collective role of the mucin family in the pathobiology of multiple malignancies to appreciate the contribution of this poorly investigated protein family.

Supplementary Material

Refer to Web version on PubMed Central for supplementary material.

Acknowledgments:

We sincerely thank Dr. Imayavaramban Lakshmanan for providing Her2 silenced CD18/HPAF cell line. We thank Jessica Mercer for editing the manuscript. We also thank the UNMC Department of Pathology for providing the patient tissue samples.

Funding.

The authors/work was partly supported by funding from the National Institutes of Health (P01 CA217798, U01 CA210240, U01 CA200466, R01 CA206444, R21 AA026428, R01 CA228524, R01 CA247471, R01 CA254036, R01 CA256973, R01 CA263575, R01 CA273349, and R44 CA235991).

Data availability statement:

All data needed to evaluate the conclusions in the paper are present in the manuscript and the Supplementary Materials.

Reference List

1. Schmid RM. Acinar-to-ductal metaplasia in pancreatic cancer development. J Clin Invest 2002; 109: 1403–1404. [PubMed: 12045253]
2. Liu J, Akanuma N, Liu C, Naji A, Halff GA, Washburn WK et al. TGF-β1 promotes acinar to ductal metaplasia of human pancreatic acinar cells. Sci Rep 2016; 6: 30904. [PubMed: 27485764]
3. Hruban RH, Goggins M, Parsons J, Kern SE. Progression model for pancreatic cancer. Clin Cancer Res 2000; 6: 2969–2972. [PubMed: 10955772]
4. Kopp JL, von Figura G, Mayes E, Liu FF, Dubois CL, Morris JPt et al. Identification of Sox9-dependent acinar-to-ductal reprogramming as the principal mechanism for initiation of pancreatic ductal adenocarcinoma. Cancer Cell 2012; 22: 737–750. [PubMed: 23201164]
5. Wei D, Wang L, Yan Y, Jia Z, Gagea M, Li Z et al. KLF4 Is Essential for Induction of Cellular Identity Change and Acinar-to-Ductal Reprogramming during Early Pancreatic Carcinogenesis. Cancer Cell 2016; 29: 324–338. [PubMed: 26977883]
6. Navas C, Hernández-Porras I, Schuhmacher AJ, Sibilia M, Guerra C, Barbacid M. EGF receptor signaling is essential for k-ras oncogene-driven pancreatic ductal adenocarcinoma. Cancer Cell 2012; 22: 318–330. [PubMed: 22975375]
7. Ardito CM, Grüner BM, Takeuchi KK, Lubeseder-Martellato C, Teichmann N, Mazur PK et al. EGF receptor is required for KRAS-induced pancreatic tumorigenesis. Cancer Cell 2012; 22: 304–317. [PubMed: 22975374]
8. Perera RM, Bardeesy N. Ready, set, go: the EGF receptor at the pancreatic cancer starting line. Cancer Cell 2012; 22: 281–282. [PubMed: 22975369]
9. Ligorio M, Sil S, Malagon-Lopez J, Nieman LT, Misale S, Di Pilato M et al. Stromal Microenvironment Shapes the Intratumoral Architecture of Pancreatic Cancer. Cell 2019; 178: 160–175.e127. [PubMed: 31155233]
10. Sandgren EP, Luetteke NC, Palmiter RD, Brinster RL, Lee DC. Overexpression of TGF alpha in transgenic mice: induction of epithelial hyperplasia, pancreatic metaplasia, and carcinoma of the breast. Cell 1990; 61: 1121–1135. [PubMed: 1693546]
11. Oliveira-Cunha M, Newman WG, Siriwardena AK. Epidermal growth factor receptor in pancreatic cancer. Cancers (Basel) 2011; 3: 1513–1526. [PubMed: 24212772]
12. Siveke JT, Crawford HC. KRAS above and beyond - EGFR in pancreatic cancer. Oncotarget 2012; 3: 1262–1263. [PubMed: 23174662]
13. Tzeng CW, Frolov A, Frolova N, Jhala NC, Howard JH, Buchsbaum DJ et al. Epidermal growth factor receptor (EGFR) is highly conserved in pancreatic cancer. Surgery 2007; 141: 464–469. [PubMed: 17383523]
14. Tomas A, Futter CE, Eden ER. EGF receptor trafficking: consequences for signaling and cancer. Trends Cell Biol 2014; 24: 26–34. [PubMed: 24295852]
15. Miaczynska M. Effects of membrane trafficking on signaling by receptor tyrosine kinases. Cold Spring Harb Perspect Biol 2013; 5: a009035. [PubMed: 24186066]
16. Hollingsworth MA, Swanson BJ. Mucins in cancer: protection and control of the cell surface. Nat Rev Cancer 2004; 4: 45–60. [PubMed: 14681689]
17. Pothuraju R, Rachagani S, Krishn SR, Chaudhary S, Nimmakayala RK, Siddiqui JA et al. Molecular implications of MUC5AC-CD44 axis in colorectal cancer progression and chemoresistance. Mol Cancer 2020; 19: 37. [PubMed: 32098629]
18. Bhatia R, Gautam SK, Cannon A, Thompson C, Hall BR, Aithal A et al. Cancer-associated mucins: role in immune modulation and metastasis. Cancer Metastasis Rev 2019; 38: 223–236. [PubMed: 30618016]

19. Gautam SK, Kumar S, Cannon A, Hall B, Bhatia R, Nasser MW et al. MUC4 mucin- a therapeutic target for pancreatic ductal adenocarcinoma. Expert Opin Ther Targets 2017; 21: 657–669. [PubMed: 28460571]
20. Kaur S, Kumar S, Momi N, Sasson AR, Batra SK. Mucins in pancreatic cancer and its microenvironment. Nat Rev Gastroenterol Hepatol 2013; 10: 607–620. [PubMed: 23856888]
21. Gurumurthy CB, O'Brien AR, Quadros RM, Adams J Jr., Alcaide P, Ayabe S et al. Reproducibility of CRISPR-Cas9 methods for generation of conditional mouse alleles: a multi-center evaluation. Genome Biol 2019; 20: 171. [PubMed: 31446895]
22. Gurumurthy CB, O'Brien AR, Quadros RM, Adams J Jr., Alcaide P, Ayabe S et al. Response to correspondence on "Reproducibility of CRISPR-Cas9 methods for generation of conditional mouse alleles: a multi-center evaluation". Genome Biol 2021; 22: 99. [PubMed: 33827648]
23. Economides AN, Frendewey D, Yang P, Dominguez MG, Dore AT, Lobov IB et al. Conditionals by inversion provide a universal method for the generation of conditional alleles. Proc Natl Acad Sci U S A 2013; 110: E3179–3188. [PubMed: 23918385]
24. Dey P, Rachagani S, Vaz AP, Ponnusamy MP, Batra SK. PD2/Paf1 depletion in pancreatic acinar cells promotes acinar-to-ductal metaplasia. Oncotarget 2014; 5: 4480–4491. [PubMed: 24947474]
25. Thompson CM, Cannon A, West S, Ghersi D, Atri P, Bhatia R et al. Mucin Expression and Splicing Determine Novel Subtypes and Patient Mortality in Pancreatic Ductal Adenocarcinoma. Clin Cancer Res 2021; 27: 6787–6799. [PubMed: 34615717]
26. Quadros RM, Miura H, Harms DW, Akatsuka H, Sato T, Aida T et al. Easi-CRISPR: a robust method for one-step generation of mice carrying conditional and insertion alleles using long ssDNA donors and CRISPR ribonucleoproteins. Genome Biol 2017; 18: 92. [PubMed: 28511701]
27. Miura H, Quadros RM, Gurumurthy CB, Ohtsuka M. Easi-CRISPR for creating knock-in and conditional knockout mouse models using long ssDNA donors. Nat Protoc 2018; 13: 195–215. [PubMed: 29266098]
28. Rachagani S, Torres MP, Kumar S, Haridas D, Baine M, Macha MA et al. Mucin (Muc) expression during pancreatic cancer progression in spontaneous mouse model: potential implications for diagnosis and therapy. J Hematol Oncol 2012; 5: 68. [PubMed: 23102107]
29. Chen NM, Singh G, Koenig A, Liou GY, Storz P, Zhang JS et al. NFATc1 Links EGFR Signaling to Induction of Sox9 Transcription and Acinar-Ductal Transdifferentiation in the Pancreas. Gastroenterology 2015; 148: 1024–1034.e1029. [PubMed: 25623042]
30. Ling S, Chang X, Schultz L, Lee TK, Chaux A, Marchionni L et al. An EGFR-ERK-SOX9 signaling cascade links urothelial development and regeneration to cancer. Cancer Res 2011; 71: 3812–3821. [PubMed: 21512138]
31. Kumar S, Torres MP, Kaur S, Rachagani S, Joshi S, Johansson SL et al. Smoking accelerates pancreatic cancer progression by promoting differentiation of MDSCs and inducing HB-EGF expression in macrophages. Oncogene 2015; 34: 2052–2060. [PubMed: 24909166]
32. Bhatia R, Bhyravbhatla N, Kisling A, Li X, Batra SK, Kumar S. Cytokines chattering in pancreatic ductal adenocarcinoma tumor microenvironment. Semin Cancer Biol 2022.
33. Ramasamy S, Duraisamy S, Barbashov S, Kawano T, Kharbanda S, Kufe D. The MUC1 and galectin-3 oncoproteins function in a microRNA-dependent regulatory loop. Mol Cell 2007; 27: 992–1004. [PubMed: 17889671]
34. Chaturvedi P, Singh AP, Chakraborty S, Chauhan SC, Bafna S, Meza JL et al. MUC4 mucin interacts with and stabilizes the HER2 oncoprotein in human pancreatic cancer cells. Cancer Res 2008; 68: 2065–2070. [PubMed: 18381409]
35. Shibata W, Kinoshita H, Hikiba Y, Sato T, Ishii Y, Sue S et al. Overexpression of HER2 in the pancreas promotes development of intraductal papillary mucinous neoplasms in mice. Sci Rep 2018; 8: 6150. [PubMed: 29670173]
36. Hsu SC, Hung MC. Characterization of a novel tripartite nuclear localization sequence in the EGFR family. J Biol Chem 2007; 282: 10432–10440. [PubMed: 17283074]
37. Hingorani SR, Petricoin EF, Maitra A, Rajapakse V, King C, Jacobetz MA et al. Preinvasive and invasive ductal pancreatic cancer and its early detection in the mouse. Cancer Cell 2003; 4: 437–450. [PubMed: 14706336]

38. Siveke JT, Schmid RM. Chromosomal instability in mouse metastatic pancreatic cancer--it's Kras and Tp53 after all. Cancer Cell 2005; 7: 405–407. [PubMed: 15894260]
39. Storz P. Acinar cell plasticity and development of pancreatic ductal adenocarcinoma. Nat Rev Gastroenterol Hepatol 2017; 14: 296–304. [PubMed: 28270694]
40. Siveke JT, Einwächter H, Sipos B, Lubeseder-Martellato C, Klöppel G, Schmid RM. Concomitant pancreatic activation of Kras(G12D) and Tgfa results in cystic papillary neoplasms reminiscent of human IPMN. Cancer Cell 2007; 12: 266–279. [PubMed: 17785207]
41. Wagner M, Weber CK, Bressau F, Greten FR, Stagge V, Ebert M et al. Transgenic overexpression of amphiregulin induces a mitogenic response selectively in pancreatic duct cells. Gastroenterology 2002; 122: 1898–1912. [PubMed: 12055597]
42. Vasseur R, Skrypek N, Duchêne B, Renaud F, Martínez-Maqueda D, Vincent A et al. The mucin MUC4 is a transcriptional and post-transcriptional target of K-ras oncogene in pancreatic cancer. Implication of MAPK/AP-1, NF-κB and RalB signaling pathways. Biochim Biophys Acta 2015; 1849: 1375–1384. [PubMed: 26477488]
43. Wang YN, Lee HH, Chou CK, Yang WH, Wei Y, Chen CT et al. Angiogenin/Ribonuclease 5 Is an EGFR Ligand and a Serum Biomarker for Erlotinib Sensitivity in Pancreatic Cancer. Cancer Cell 2018; 33: 752–769.e758. [PubMed: 29606349]
44. Kitai Y, Iwakami M, Saitoh K, Togi S, Isayama S, Sekine Y et al. STAP-2 protein promotes prostate cancer growth by enhancing epidermal growth factor receptor stabilization. J Biol Chem 2017; 292: 19392–19399. [PubMed: 28986450]
45. Al-Akhrass H, Naves T, Vincent F, Magnaudeix A, Durand K, Bertin F et al. Sortilin limits EGFR signaling by promoting its internalization in lung cancer. Nat Commun 2017; 8: 1182. [PubMed: 29084952]
46. Lakshmanan I, Seshacharyulu P, Haridas D, Rachagani S, Gupta S, Joshi S et al. Novel HER3/MUC4 oncogenic signaling aggravates the tumorigenic phenotypes of pancreatic cancer cells. Oncotarget 2015; 6: 21085–21099. [PubMed: 26035354]
47. Engle DD, Tiriac H, Rivera KD, Pommier A, Whalen S, Oni TE et al. The glycan CA19-9 promotes pancreatitis and pancreatic cancer in mice. Science 2019; 364: 1156–1162. [PubMed: 31221853]
48. Hezel AF, Gurumurthy S, Granot Z, Swisa A, Chu GC, Bailey G et al. Pancreatic LKB1 deletion leads to acinar polarity defects and cystic neoplasms. Mol Cell Biol 2008; 28: 2414–2425. [PubMed: 18227155]
49. Harms DW, Quadros RM, Seruggia D, Ohtsuka M, Takahashi G, Montoliu L et al. Mouse Genome Editing Using the CRISPR/Cas System. Curr Protoc Hum Genet 2014; 83: 15.17.11–27.
50. Kumar S, Das S, Rachagani S, Kaur S, Joshi S, Johansson SL et al. NCOA3-mediated upregulation of mucin expression via transcriptional and post-translational changes during the development of pancreatic cancer. Oncogene 2015; 34: 4879–4889. [PubMed: 25531332]
51. Gruber R, Panayiotou R, Nye E, Spencer-Dene B, Stamp G, Behrens A. YAP1 and TAZ Control Pancreatic Cancer Initiation in Mice by Direct Up-regulation of JAK-STAT3 Signaling. Gastroenterology 2016; 151: 526–539. [PubMed: 27215660]
52. Ganguly K, Bhatia R, Rauth S, Kisling A, Atri P, Thompson C et al. MUC5AC serves as the nexus for β-catenin/c-Myc interplay to promote glutamine dependency during pancreatic cancer chemoresistance. Gastroenterology 2021.
53. Bhatia R, Muniyan S, Thompson CM, Kaur S, Jain M, Singh RK et al. Neutrophil Gelatinase-Associated Lipocalin Protects Acinar Cells From Cerulein-Induced Damage During Acute Pancreatitis. Pancreas 2020; 49: 1297–1306. [PubMed: 33122517]

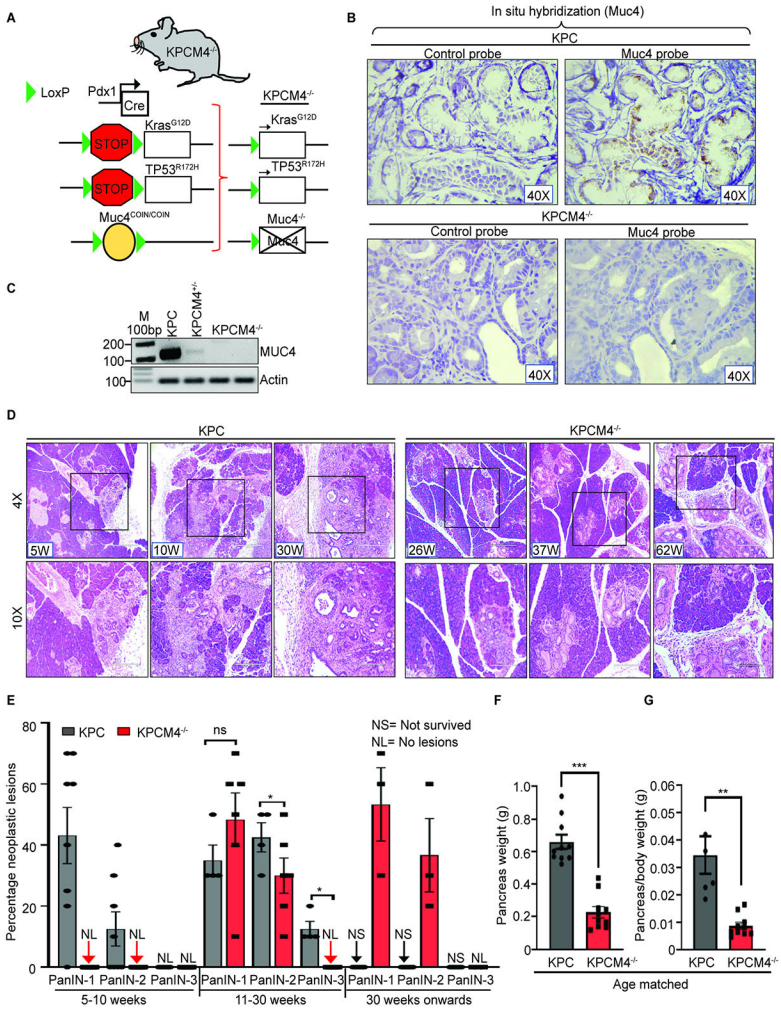

Figure 1. The Muc4 depletion delays the initiation of PDAC.

A. The generation of conditional murine models expressing mutant Kras$^{-/+LSLG12D}$; TP53$^{-/+LSLR172H}$ and pancreas-specific Muc4 deletion (COIN) upon Pdx-1-Cre-based recombination. **B.** The *in-situ* hybridization confirmed the absence of Muc4 transcripts in the early pancreatic lesions (PanIN) of the KPCM4$^{-/-}$ murine model. **C.** Reverse transcriptase-PCR (RT-PCR) from the cDNA derived from heterozygous and homozygous cell lines generated from KPC and KPCM4$^{-/-}$ murine models, showing successful Muc4 depletion after Cre activation. **D.** The H&E staining of KPC and KPCM4$^{-/-}$ pancreatic tissues demonstrated the delay in the onset of PanIN lesions. **E.** The percentage of different stages of PanIN lesions in the KPC (n=8) and KPCM4$^{-/-}$ (n=6, 11-30 weeks; n=3 above 30 weeks) murine models (NL: No lesions, NS: Not survived). **F, G.** The significant differences in the pancreas weight (F) and pancreas weight by body weight (G) in KPC and KPCM4$^{-/-}$ murine models. (n=10 each). The data in panels F to G are presented as mean ± SEM. *p<0.05, **p<0.01, ***p<0.001.

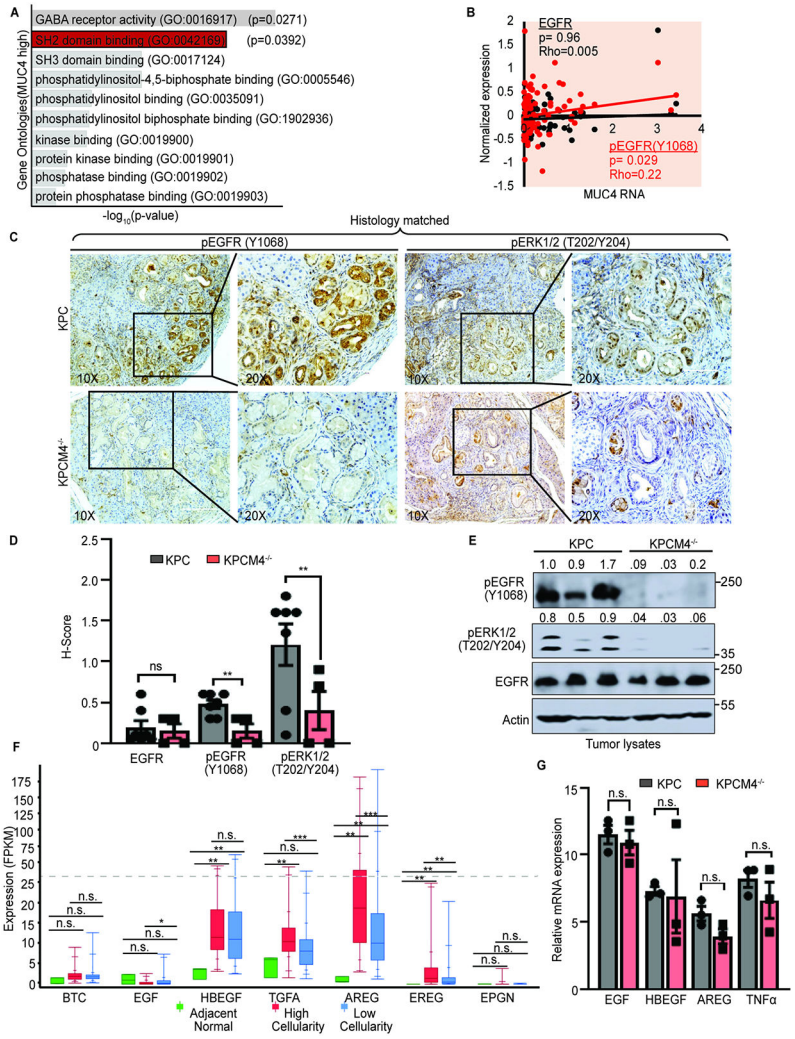

Figure 2. The early lesions in the pancreatic tissues of KPCM4$^{-/-}$ mice display significantly lower EGFR and ERK1/2 phosphorylation status.

A. Gene ontology analysis showed the enrichment of tyrosine kinase-dependent cascades in the high MUC4 expressing group in the pancreatic cancer TCGA dataset (https://maayanlab.cloud/ Enrichr/). **B.** A correlation between MUC4 transcripts from the TCGA dataset and the matched reverse-phase proteomic data for the levels of EGFR and pEGFR (Y1068) (p=0.96; Rho 0.005 for EGFR and p=0.029; Rho= 0.22 for pEGFR) in the PDAC tissues. **C, D.** The IHC (C) and H-score (D) analysis showed a significantly reduced EGFR and ERK1/2 phosphorylation in the early PanIN lesions of the KPCM4$^{-/-}$ murine model in the histology-matched KPC and KPCM4$^{-/-}$ samples. (KPC n=7 and KPCM4$^{-/-}$ n=4). **E.** Immunoblotting analysis for the levels of pEGFR(Y1068) and pERK1/2(T202/Y204) in the lysates of pancreatic tissue isolated from KPC and KPCM4$^{-/-}$ murine models. **F.** The expression profile of different EGFR-ligands in PDAC tissues from the TCGA dataset (n=140) with high and low epithelial cellularity. **G.** The relative mRNA expression of different EGFR-ligands in the KPC and KPCM4$^{-/-}$ mouse pancreatic tissues. (n=3). The data in panels D and G are presented as mean ± SEM. *p<0.05, **p<0.01, ***p<0.001.

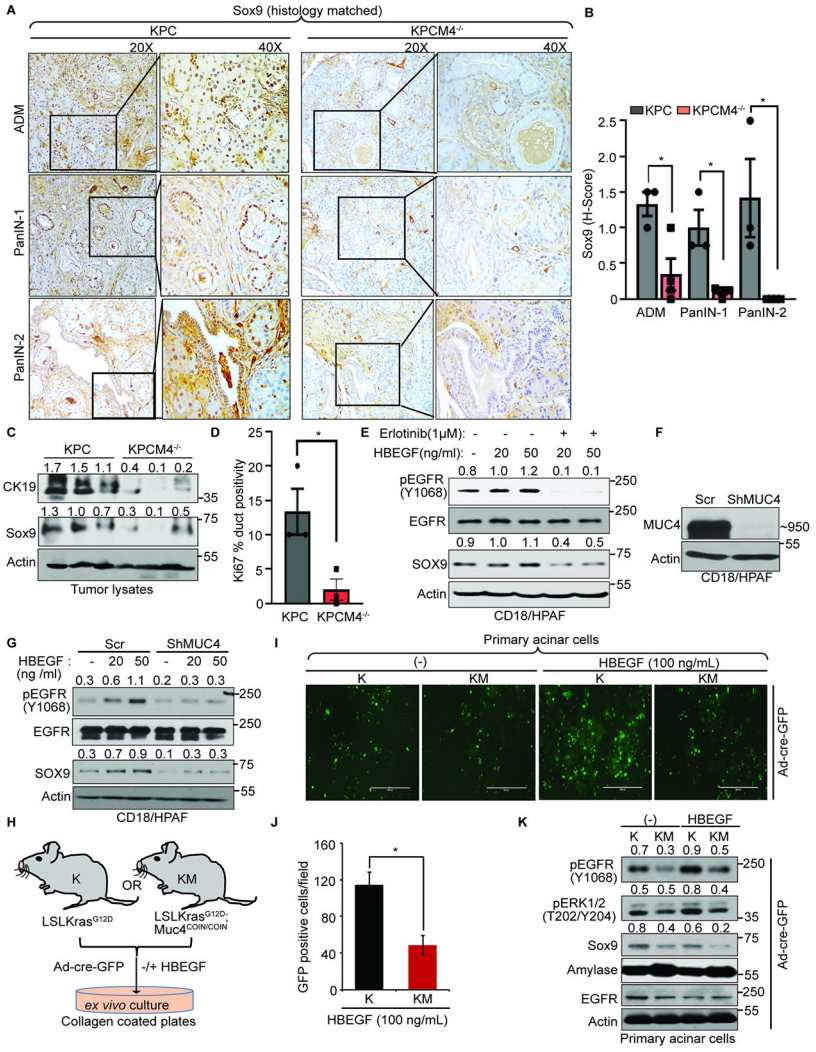

Figure 3. The Muc4 depletion significantly reduces acinar-to-ductal metaplasia (ADM) in mouse pancreatic tissues.

A, B. The IHC and H-score analysis for Sox9 expression in ADM, PanIN-1, and PanIN-2 lesions in the histology-matched pancreatic tissues from KPC and KPCM4$^{-/-}$ murine models. **C.** Immunoblotting analysis demonstrated the reduced expression of CK19 and Sox9 in the lysates of pancreatic tissues isolated from the KPC and KPCM4$^{-/-}$ murine models. **D.** The percentage Ki67 ductal positivity in the nuclei of histology-matched pancreatic tissues isolated from KPC and KPCM4$^{-/-}$ murine models. **E.** The immunoblotting analysis demonstrated the reduction in SOX9 expression after EGFR inhibition by Erlotinib in the human PDAC cell line. **F.** Validation of shRNA-mediated stable knockdown of MUC4 expression in PDAC cells. **G.** Immunoblotting analysis showed a decrease in SOX9 expression in MUC4 KD cells treated with different concentrations of HBEGF. **H.** Schematic representation of isolation of primary pancreatic acini isolated from Kras$^{-/+LSLG12D}$ (K) and Kras$^{-/+LSLG12D}$; Muc4$^{COIN/COIN}$ (KM) murine models for *ex vivo* experiments. **I, J.** Isolated primary acinar cells cultured for 5-days with mHBEGF (100 ng/ml) were transduced with Ad-Cre-GFP expressing viral particles and analyzed for the

ductal structures (GFP positive ductal structures). **K**. The immunoblotting analysis showed the reduced phosphorylation status of EGFR, ERK1/2, and Sox9 expression in the pancreatic acini isolated from KPM4$^{-/-}$ compared to KP murine models transduced with Ad-Cre-GFP virus. The amylase expression was used as a marker for the acinar cells. The data in panels B, D, and J are presented as mean ± SEM. *p<0.05.

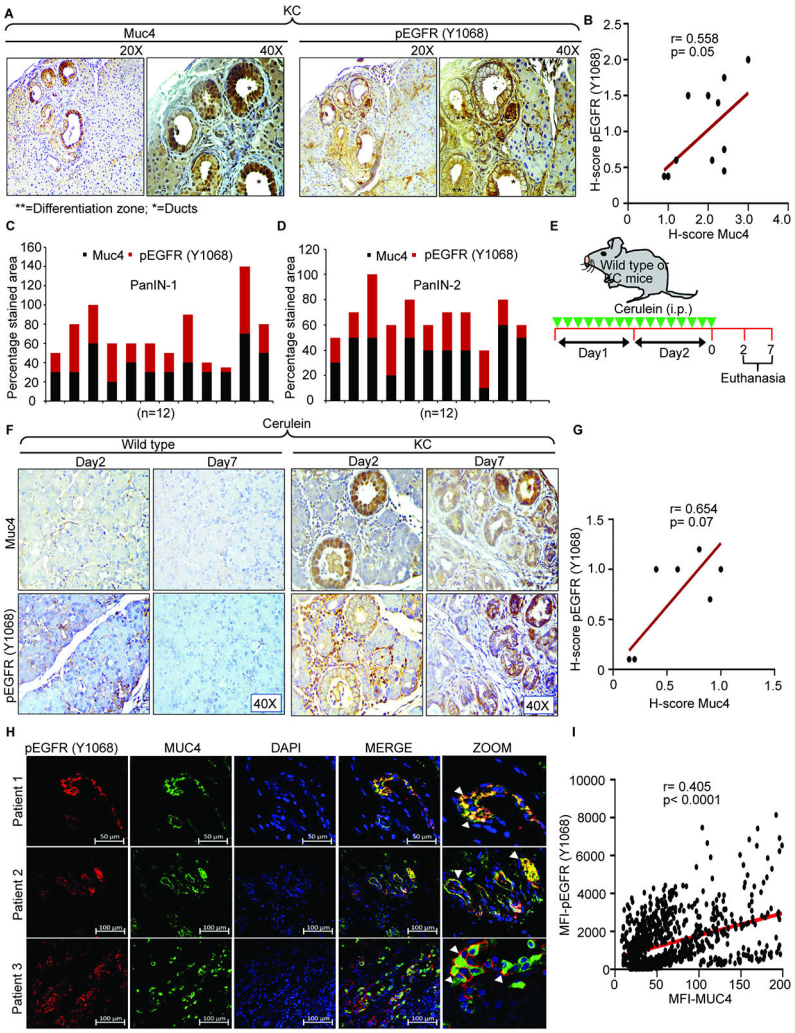

Figure 4. Muc4 expression shows a significant correlation with EGFR activity in the differentiating ductal lesions in the pancreatic tissues.

A. The IHC analysis for the Muc4 and pEGFR co-expression in the early transdifferentiating ducts/PanIN lesions of KC tissues. **B.** The H-score analysis demonstrated a significant correlation between Muc4 and pEGFR (Y1068) co-expression in the transdifferentiating ducts in the pancreas. **C, D.** Pearson correlation between Muc4 and pEGFR (Y1068) co-expression in PanIN-1 (C), and PanIN-2 (D) lesions. **E.** Schematic representation of cerulein (75 μg/kg body weight) intraperitoneal injections following staggered protocol for the accelerated PanIN lesion formation. **F.** The increased Muc4 and pEGFR (Y1068) co-expression in cerulein-treated day 2- and 7- KC mice pancreas. **G.** A strong correlation between Muc4 and pEGFR (Y1068) co-expression in the pancreas (Pearson correlation=0.654) of KC mice upon cerulein administration. **H, I.** The MUC4 and pEGFR (Y1068) expression and co-localization, and quantification in PDAC patient tissues by immunofluorescence.

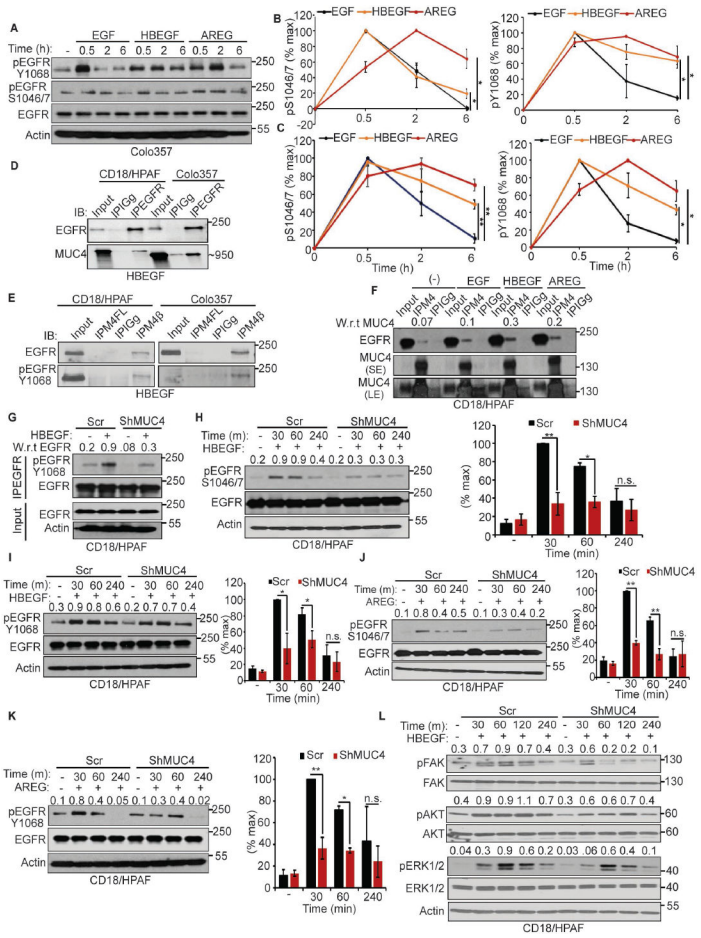

Figure 5. MUC4 interacts with EGFR upon ligand stimulation leading to sustain signaling.

A. The Colo357 cells were treated with 10ng/ml of human EGF, HBEGF, and AREG and analyzed for EGFR phosphorylation. **B, C.** Quantification of EGFR activation at Y1068 and S1046/7 residues. Percentage activation by each ligand at indicated time points as the function of the maximum intensity by each ligand in Colo357 (B) CD18/HPAF (C) PDAC cells. **D.** CD18/HPAF and Colo357 cells were treated with HBEGF (100 ng/ml; 5 min) and analyzed for MUC4 co-immunoprecipitation with EGFR. **E.** Reciprocal co-immunoprecipitation of EGFR and pEGFR (Y1068) with MUC4 after treatment with HBEGF (100 ng/ml). **F.** Comparative analysis of EGFR co-immunoprecipitation with MUC4 upon stimulation with different EGFR-ligands. **G.** The EGFR immunoprecipitation in MUC4-proficient and -deficient cells treated with HBEGF (100 ng/ml) and analyzed for pEGFR levels. **H, I.** The CD18/HPAF MUC4-Scr and KD PDAC cells were analyzed for the difference in EGFR phosphorylation status at S1046/7 (H) and Y1068 (I) residues upon HBEFG (10 ng/ml) treatment. **J, K.** The CD18/HPAF MUC4-Scr and KD PDAC cells were analyzed for the difference in EGFR phosphorylation status at S1046/7 (J) and Y1068 (K) residues upon AREG (10 ng/ml) treatment. **L.** Higher EGFR downstream signaling in CD18/HPAF PDAC cells in the MUC4 proficient than the deficient cells. The data in panels B, C, H, I, J, and K are presented as mean ± SEM. *p<0.05, **p<0.01.

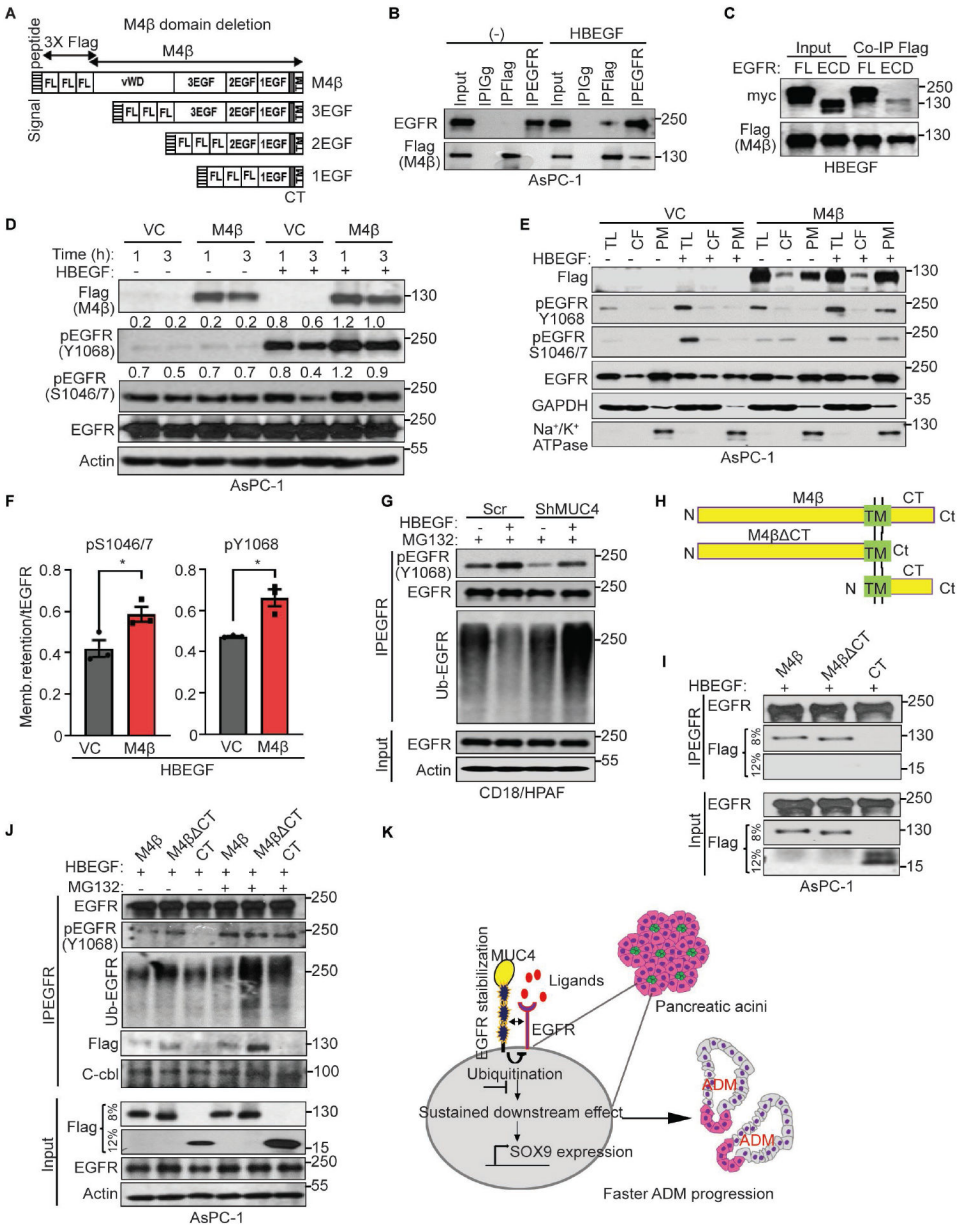

Figure 6. MUC4 expression maintains EGFR activity by preventing its ubiquitination upon ligand stimulation.

A. Schematic representation of MUC4β domain-deletion constructs cloned in a 3XflagCMV9 plasmid**. B.** The co-IP of Flag-tagged MUC4β with EGFR in the MUC4β overexpressing PDAC cell line, AsPC-1. **C.** The co-IP of myc-tagged full-length (FL) and extracellular domain (ECD) of EGFR with Flag-tagged MUC4β overexpressed in AsPC-1 PDAC cells. **D.** The AsPC-1 PDAC cells overexpressing Flag-tagged MUC4β were analyzed for EGFR phosphorylation at Y1068 and S1046/7 residues at the indicated time points**. E, F.** Immunoblotting analysis and quantification of MUC4β-stabilized EGFR expression on the plasma membrane in the AsPC-1 PDAC cells, overexpressing Flag-tagged MUC4β. TL: total lysate, CF: cytoplasmic fraction, PM: plasma membrane fraction. **G.** The EGFR IP from MUC4-Scr and KD CD18/HPAF PDAC cells after pretreatment

with 30μM of proteasome inhibitor MG132, 2h prior to HBEGF treatment, was probed with ubiquitin antibody. **H.** Schematic representation of MUC4β and N-terminal domain deletions constructs consisting of MUC4βΔCT (no cytoplasmic tail) and MUC4-CT (only cytoplasmic tail), respectively. **I.** The co-IP of MUC4β and MUC4βΔCT with EGFR in ASPC-1 PDAC cells overexpressing the indicated constructs after treatment with the HBEGF. The EGFR failed to co-IP the MUC4-CT. **J.** The EGFR IP from the MUC4β, MUCβΔCT, and CT overexpressing constructs in AsPC-1 PDAC cells after pretreatment with 30μM of MG132, 2h prior to HBEGF treatment. The IP fractions were probed with pEGFR (Y1068), ubiquitin, and c-Cbl antibodies. **K.** Schematic representation depicting MUC4 interaction and stabilization of EGFR on the plasma membrane and its sustained activity upon ligand stimulation during PDAC initiation. The data in panel F is presented as mean ± SEM. *p<0.05.